

# Fitting the Bragg peak for accurate proton range determination

Koen Lambrechts

July 10, 2015

## **Abstract**

This paper focusses on the uncertainties in proton range determination in the framework of optimizing proton therapy planning. In particular the dependency of proton range determination on the reference position at the distal edge of the Bragg peak is investigated.

# Contents

<b>1</b>	<b>Introduction</b>	<b>3</b>
1.1	Advantages of proton therapy . . . . .	3
1.2	Physics of proton therapy . . . . .	4
1.3	Determining the Range . . . . .	5
1.4	Improving testing of the model . . . . .	6
<b>2</b>	<b>Method</b>	<b>7</b>
2.1	Data and sample's used . . . . .	7
2.2	Finding a fit to the data . . . . .	9
2.3	Evaluating the fit . . . . .	10
2.4	Comparing $\Delta R$ . . . . .	11
<b>3</b>	<b>Results</b>	<b>11</b>
3.1	Parameters and errors for the fitted functions . . . . .	11
3.2	$\Delta R$ . . . . .	14
<b>4</b>	<b>Discussion and conclusions</b>	<b>17</b>
<b>5</b>	<b>References</b>	<b>19</b>

# 1 Introduction

The idea of proton radiation as a method to treat cancer has been around ever since Robert Wilson's first publication on the topic in 1946. In the forty years following Wilson's publication proton therapy was applied, but only in a very limited amount of cases, about ten thousand, over these forty years, and without specific equipment built for this purpose. This changed in 1990 when the James M. Slater Proton Treatment and Research Center was opened in Loma Linda California. At this hospital-based facility all kind of cancers could be treated with the help of proton therapy. This milestone event marked the start of an increased investment in proton therapy, resulting in a growth of the amount of patients treated up to about a hundred thousand today[6]. This number is expected to rise, especially since there is still room for improvement of proton therapy, making it applicable in even more situations.

One of the locations where research on these improvements is done is Groningen. In February 2015 the construction of a hospital-based proton therapy treatment centre at the Universitair Medisch Centrum Groningen was announced, the first of its kind in the Netherlands. Apart from treating patients, the UMCG will also collaborate with KVI-CART in research on proton therapy. The focus of this research is on improving methods to acquire relevant patient information and on using this information to optimize treatment planning and minimize the dose to the surrounding tissue. Alongside Groningen, a second facility will be build in Delft and most likely a third and fourth will follow in Maastricht and Amsterdam.

## 1.1 Advantages of proton therapy

On comparing proton therapy with photon therapy, the current dominant form of radiation therapy, the advantages of proton therapy present themselves instantly. A glance at the depth profiles for proton and photon dose in figure 1 shows that the depth dependency is very different for these two types of radiation. The dose deposited by a photon beam falls off as the beam penetrates deeper into the tissue, this means that for a single beam the highest dose is deposited just after the position of entrance into the body. From this moment on the dose deposition decreases with depth but never falls to zero. This implies that apart from irradiating the tumour, a photon beam irradiates a significant amount of surrounding tissue as well.

The profile of the mono-energetic proton beam shows that for these beams the dose deposition is relatively low at entrance of the body and slowly builds up to a sharp peak that quickly falls off to zero after it reaches its maximum. In general this peak, which is called a Bragg peak, implies that accurate knowledge of the position of this peak in the tissue allows physicians to deliver the highest radiation precisely in the tumour. Proton therapy can therefore spare much more of the surrounding tissue than photon therapy. An unique feature of

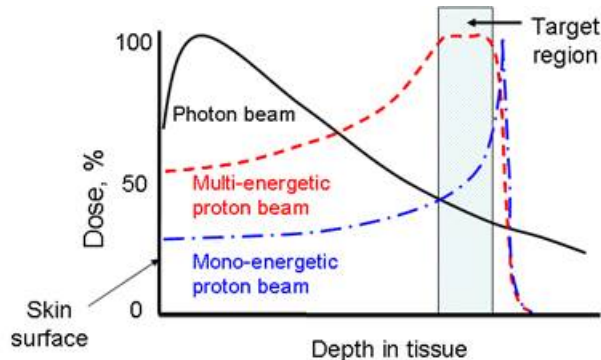


Figure 1: Schematic picture of the energy deposition of proton, multi-energetic proton and photon beams as a function of depth in the tissue. The dose is given relative to the maximum dose.

proton therapy is the possibility of treating tumours that are positioned close to radio sensitive tissue such as the heart. The fact that almost instantly after the maximum in the dose-depth profile is reached, the dose drops to zero ensures that tissue 'behind' the tumour is not effected by the radiation. This is not possible for photon therapy since the photon beam still delivers doses after surpassing the target region. As already mentioned, all these advantages depend on accurate knowledge of the position of the Bragg peak and this issue will be discussed further on in this paper[5].

## 1.2 Physics of proton therapy

The energy deposition of the proton beam and the proton range, which is the average distance a proton travels before coming to rest, are determined by the mass stopping power ( $\text{MeVcm}^2\text{g}^{-1}$ ) of the tissue that it traverses as given by

$$\frac{S}{\rho} = -\frac{dE}{\rho dx} \quad (1)$$

where  $S$  is the linear stopping power,  $\rho$  is the mass density ( $\text{cm}^{-2}\text{g}$ ) of the traversed material and  $\frac{dE}{dx}$  is the energy deposition per unit of length ( $\text{MeVcm}^{-1}$ ).

We can identify three main interaction mechanisms that make up the stopping power. The first, and most dominant in determining the shape of the Bragg peak, are electromagnetic proton-electron-interactions. These electromagnetic interactions between protons from the proton beam and atomic electrons from the human tissue, only slightly influence the direction of the beam, but they do take away a little bit of the total proton energy on every interaction. The

amount of energy involved in each interaction increases with duration of the interaction. Since the proton loses energy and thus speed as it moves through the tissue, the duration of the interaction increases. This results in much greater loss of energy towards the end of the proton range.

A second, less energy exchange efficient interaction, is electromagnetic scattering of the beam-protons on atomic nuclei, so called multiple Coulomb scattering [MCS]. The deflection of a proton by a single atomic nucleus is in general small, but the series of random deflections causes the protons to scatter Gaussian along the axis of incident. The effect that this has on the Bragg peak can be imagined by looking at the human body in an xyz-frame while defining the depth in tissue along the x-axis. (which is the axis of incident). Assuming now that all protons have the same average range, it is easy to imagine that deflected protons will not reach the same depth in tissue as non deflected protons. This results in broadening of the Bragg peak along the x-axis.

The third important process underlying the stopping power is the non-elastic collisions between primary protons and atomic nuclei. In this case the primary protons knocks several nucleons out of the nucleus, thereby causing a full energy deposit in the region of the collision. This happens to about 20% of 160 MeV protons, which results in a loss of about 1% of the total protons in a beam per centimetre in human tissue.

### 1.3 Determining the Range

To improve proton therapy and allow for more accurate and precise treatment planning, more accurate knowledge of the proton range in patients is necessary. The problem with acquiring information about this range in the patient is that there is, at this point, no direct method to determine the range or stopping power. Up until now CT scans and models to link the Hounsfield units from CT scans to  $S$  have been used, but the uncertainties in determining  $S$  originates from the lack of a one-to-one mapping of these two parameters. Improvement of the model linking these two parameters could decrease uncertainties in estimates of  $S$  and thus proton range.

The accuracy of such a model can be checked by making predictions for the stopping power of materials based on information from a CT scan. This prediction can then be checked by measuring the actual stopping power in an experimental set-up. For convenience, stopping power is usually expressed as water equivalent thickness (WET). The WET is the thickness of water that is needed to result in the same stopping, as is shown in figure 2. Taking water as the standard makes sense since water is the main constituent of the human body. The uncertainties in the determination of range difference  $\Delta R$  as defined in figure 2 will be the main focus of this thesis.

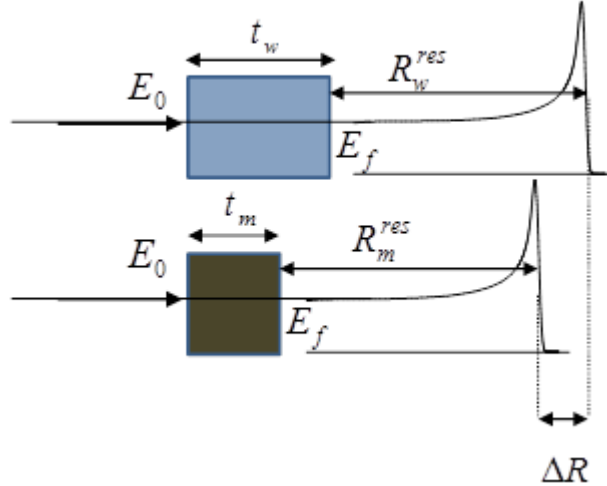


Figure 2: Definition of water equivalent thickness of a material with thickness  $t_m$  as the thickness of water  $t_w$  that results in an equal residual range of that of the material ( $R_m^{res} = R_w^{res}$ ).  $E_0$  and  $E_f$  are energy at the start and end of the material and  $\Delta R$  is the difference in range

The fact that this is a convenient concept is shown in this experimental set-up shown in figure 2. In this experiment the same piece of material that has already been scanned in a CT scanner is placed inside of a tank of water. In front of the material the KVI-CART AGOR cyclotron emits a continuous beam of protons, so a constant beam of protons is sent through the material into the water tank. Using a dose meter one can now measure the energy deposited as a function of depth in water, which is defined by the stopping power. Both the modelling of results of the CT scan and the direct energy dose measurement result in an energy deposited to depth dependency with its characteristic Bragg peak as in figure 1. By comparing these two graphs, we can determine how well the model translates the CT scan into actual stopping power.

#### 1.4 Improving testing of the model

To find the WET of a certain material, the depths of the measured Bragg peaks are compared, resulting in a  $\Delta R$  that expresses the difference in depth between a Bragg peak in water only and a Bragg peak after traversing a certain thickness of material. This seems very sensible, but it is not the complete story. The concept of the Bragg peak is very well understood, and can be explained by the physics mentioned above, but this does not mean that every detail of the Bragg peak is known. This lack of understanding brings up an important question

with respect to comparison of these measured Bragg peaks, namely which point of the Bragg peaks should be compared. Although thus far an argument has been made for taking 80% of the maximum height at the distal side of the Bragg peak as point of comparison, no quantitative test has been performed[4]. In this study the effect of determining the distance between a Bragg peak in water and a Bragg peak traversing a certain thickness of an other material at different heights will be researched.

## 2 Method

To be able to say something sensible about the impact of the chosen height of the Bragg peak to determine the water equivalent thickness of a material, it is crucial to have a well defined set of Bragg peaks to work with. The method used in this research is one where a function is fitted to six measured Bragg peaks. This fit can then be used to find the depth at which the Bragg peak has 100%, 90%, 80% etc. of its maximum height. This fit is crucial since the data sets do not form a continuous set but is in equally sized spatial bins of 0.2 mm, so that for example the exact 80% position is most likely not in the data set.

### 2.1 Data and sample's used

The Bragg peaks are measured using a dosimeter that measures the dose deposition as a function of depth of a proton beam averaged over an interval of 0.2 mm around the area of interest. The set-up used for this experiment can be seen in figure 3. The construction of a function that fits this data will be done for a Bragg peak in water, but five more Bragg peaks are analysed of which the material is placed at about 50mm from the entrance window of the water tank. The properties of the material samples are listed in table 1 and the ranges measured are typically about 200-250 mm.

Table 1: This table shows the properties of the materials used in the experiment, with  $\rho$  the mass density and  $\frac{\rho_e}{\rho_e^w}$  the electron density relative to water

	Thickness (mm)	$\rho$ (g/cm <sup>-3</sup> )	$\frac{\rho_e}{\rho_e^w}$ (e/cm <sup>-3</sup> )
Water		0.998	1.000
Fat	22.017	0.946	0.929
Bone	12.941	1.823	1.699
Solid water	19.985	1.045	1.017
Aluminium	8.957	2.691	2.341
Lung	46.977	0.428	0.418

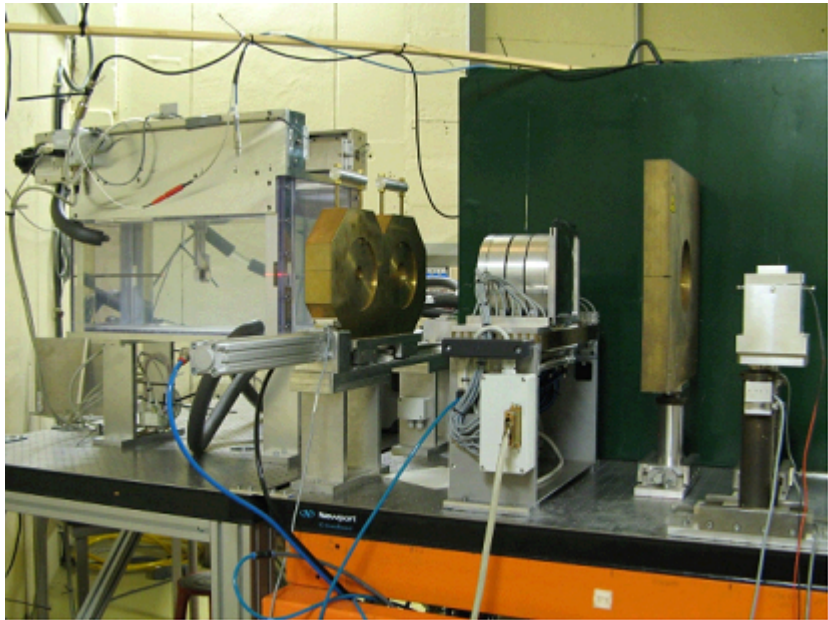


Figure 3: In this set-up the proton beam comes in from the right side, entering at a determined energy into the water tank where the dose is measured as described above. A piece of material can be put in the water tank at a preferred distance to the point of entrance of the beam.



## 2.2 Finding a fit to the data

Finding a function that fits nicely to the full dataset collected in the experiment mentioned is very difficult and actually requires a function that predicts the precise dose profile of the protons. A description of the part on the right side of the maximum dose deposition would however suffice in this research since only points on this side of the maximum have to be compared. This eases up the task a lot and it allows for example for a function with a sum of 3 Gaussians shown in equation 2.

$$D(x) = a_1 e^{-\left(\frac{x-b_1}{c_1}\right)^2} + a_2 e^{-\left(\frac{x-b_2}{c_2}\right)^2} + a_3 e^{-\left(\frac{x-b_3}{c_3}\right)^2} \quad (2)$$

Here  $D$  is the dose,  $x$  is the depth (in mm) and  $a_{1,2,3}$ ,  $b_{1,2,3}$  and  $c_{1,2,3}$  are free parameters. This function results in a squared error (SSE) of the order  $10^{-6}$  for the data points up to 7 mm left of the maximum and down to almost zero to the right of the maximum. The error is small enough, but the number of parameters makes it difficult to really understand any changes that the function undergoes when it is fitted to a slightly different Bragg peak.

The Gaussian shape of the Bragg peak hints to a Gaussian-like function as a good trial fit, but a critical look at a Bragg peak reveals that the shape is not completely Gaussian, specifically the part on the left of the maximum does not follow a Gaussian. This was noticed for neutron Bragg peaks by Boualem Hammouds and he proposed a modified Gaussian as a fit function, using 3 parameters[2]. A slightly changed version of this function is shown in equation 3

$$D(x) = \alpha e^{\frac{\tau^2 \sigma^2}{2} + \tau(x-\mu)} \text{Erfc}\left(-\frac{\mu-x}{\sigma\sqrt{2}} + \frac{\tau\sigma}{\sqrt{2}}\right) \quad (3)$$

where  $x$  is the depth in tissue (in mm),  $\alpha$ ,  $\tau$ ,  $\sigma$  and  $\mu$  are the parameters to be fitted and Erfc is the error function defined in equation 4 .

$$\text{Erfc}(z) = 1 + \frac{2}{\sqrt{\pi}} \int_0^z dx e^{-x^2} \quad (4)$$

In a normal Gaussian the  $\alpha$  would determine the height of the Gaussian, the  $\sigma$  would give the standard deviation and the  $\mu$  would be the 'x' value where the Gauss reaches its maximum and. These parameters should behave more or less, but not exactly, the same with the addition of the  $\tau$  that does not occur in the normal Gaussian but which determines the manipulation of the left side of the Gaussian in the modified Gaussian.

Table 2: The Root Mean Square Errors (RMSE) as a function of the bin number for the maximum at bin 128.

Bin number	RMSE
181	$9.32 * 10^{-5}$
186	$1.042 * 10^{-4}$
191	$1.056 * 10^{-4}$
196	$1.115 * 10^{-4}$
201	$1.186 * 10^{-4}$
206	$1.166 * 10^{-4}$

Table 3: The Root Mean Square Errors (RMSE) as a function of the bin number for the maximum at bin 128 and 63 bins to the right of the maximum.

Bin number	RMSE
128	$1.066 * 10^{-4}$
127	$1.058 * 10^{-4}$
126	$1.052 * 10^{-4}$
125	$1.044 * 10^{-4}$
124	$1.037 * 10^{-4}$
123	$1.030 * 10^{-4}$
122	$1.023 * 10^{-4}$
121	$1.015 * 10^{-4}$
120	$1.029 * 10^{-4}$
119	$1.032 * 10^{-4}$
118	$1.056 * 10^{-4}$
117	$1.111 * 10^{-4}$

### 2.3 Evaluating the fit

The function in equation 3 proves to be a good fit for the Bragg peaks used in this research but since not all data points are used for this fit, a standard interval of data points to be included has to be established. The points to the right of the maximum have very little effect on the parameters, so a quick scan of which the results are shown in table 2, shows that 63 data points to the right of the maximum is good. The RMSE is the 'root mean squared error', or:  $RMSE = \sqrt{\frac{SSE}{n-m}}$  with  $n$  the number of data points included  $m$  the number of parameters used and SSE the sum of squared errors.

A more thorough analysis with the 63 points to the right of the maximum of the effect of the amount of points left of the maximum, shown in table 3, indicates that seven data points yields the lowest RMSE. This number of data points, 7 to the left and 63 to the right of the maximum and thus 71 in total, is used for the rest of this research.

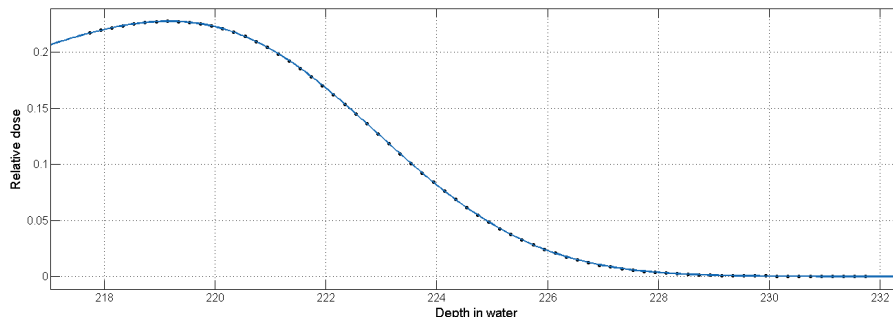


Figure 4: The fit for the Bragg peak in water with 71 data points with relative dose as WDBins and depth in water (mm) as WXBins

## 2.4 Comparing $\Delta R$

Fits to the sets of data for the different materials are found using the fixed amount of data points mentioned and the trial function from equation 3. This results in a fit as shown in figure 4. The errors for these fits are of the same order as the errors for the fit of the data set in water. The distances between the Bragg peak in water and a Bragg peak after the beam traversed a certain distance through a material at various heights of the Bragg peaks are now determined by calculating the 'x' for the fit for each of the Bragg peaks for maximum height, 90%, 80%, 70%, 60%, 50%, 40%, 10% and 1% of the maximum height. The main goal is to find an answer to the question whether it makes a difference at what height of the Bragg peak the distance ( $\Delta R$ ) between two Bragg peaks is measured. Therefore the Bragg peak in water can safely be used as the Bragg peak to compare the distances of all other Bragg peaks to.

## 3 Results

### 3.1 Parameters and errors for the fitted functions

Table 4 shows the acquired parameters for equation 3 for different materials. What can be seen is that the parameters are, as expected of the same order for all materials.

In figure 5 all parameters are rescaled to fit into a single plot, but the relative differences for a certain parameter are maintained. In this figure the parameters are plotted as a function of density. The parameters differ but not systematic, at least not when comparing the first 5 materials. This can be shown by comparing the value for  $\mu$  and  $\tau$  for fat, bone and aluminium. The  $\mu$  for these materials is ranked from smaller to bigger aluminium < bone < fat, however

Table 4: The parameters for the function that is fitted to the Bragg peaks in water, fat, bone, solid water, aluminium and lung.

Material	$\alpha$	$\tau$	$\sigma$	$\mu$
Water	0.1748	0.09731	2.403	222.5
Fat	0.1761	0.09928	2.449	223.7
Bone	0.1748	0.09703	2.405	214.7
Solid water	0.1732	0.09599	2.422	222.3
Aluminium	0.1764	0.09836	2.425	212.8
Lung	0.1637	0.08655	2.921	249.8

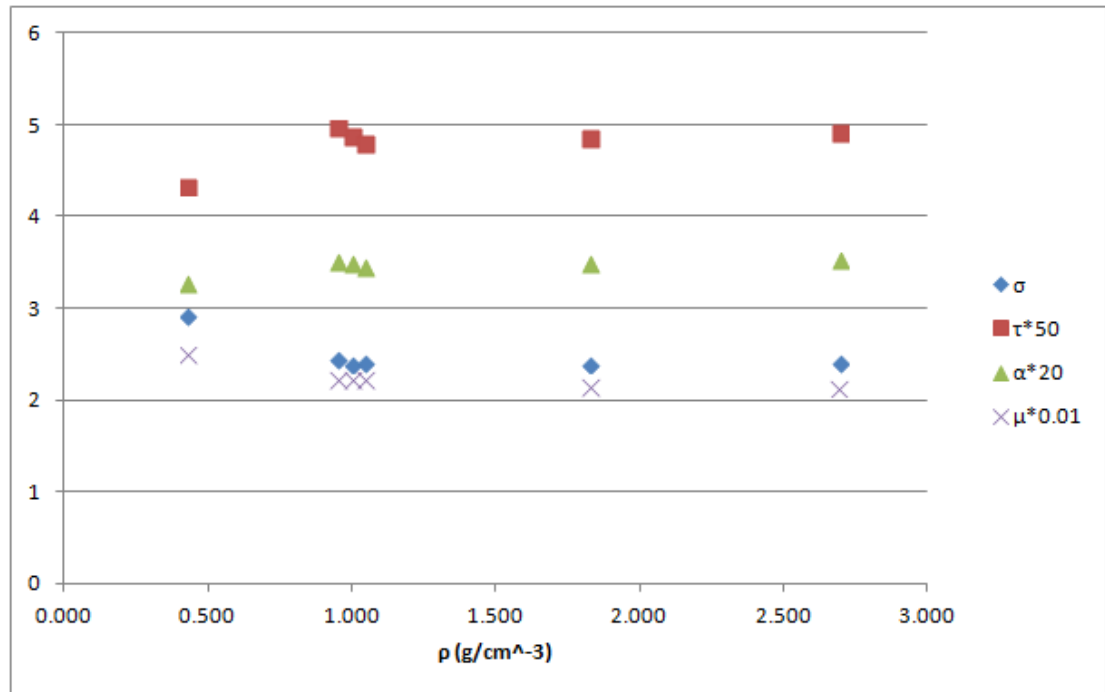


Figure 5: Fit parameters plotted as a function of the mass density of the material that was traversed by the proton beam.

Table 5: The Root Mean Square Errors (RMSE) for the functions fitted to the Bragg peaks in different materials.

Material	RMSE
Water	$8.911 \cdot 10^{-5}$
Fat	$9.19 \cdot 10^{-5}$
Bone	$1.18 \cdot 10^{-4}$
Solid water	$9.975 \cdot 10^{-5}$
Aluminium	$1.87 \cdot 10^{-4}$
Lung	$2.479 \cdot 10^{-4}$

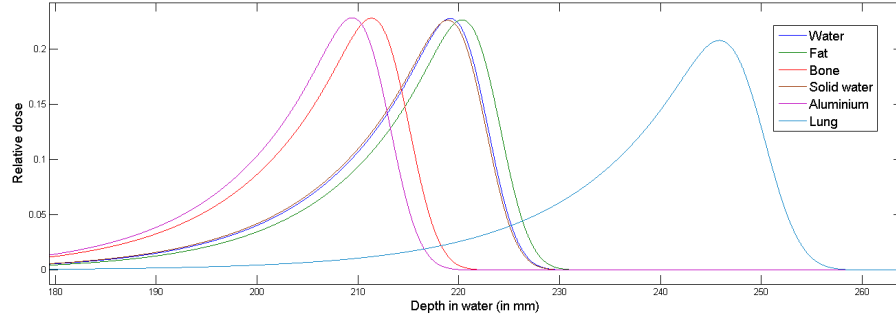


Figure 6: Relative dose deposition as a function of depth water after the proton beam traversed the sample materials: water, fat, bone, solid water, aluminium and lung.

the  $\tau$  for these materials from smaller to bigger is bone < aluminium < fat. So it seems that there is no well defined link between the material and the parameters. Comparing the parameters of the function for the lung Bragg peak to the other parameters gives some more insight. The Bragg peak for lung is described by a much bigger  $\mu$ , a much smaller  $\tau$  and  $a$ , which should effect the height of the function, and a much bigger  $\sigma$  which implies a much larger spread of the Bragg peak. This is indeed confirmed in figure 6.

Table 5 shows the RMSE in the fits for all 6 materials used in this research. The RMSE translates to a SSE of order  $10^{-6}$  or  $10^{-7}$ , which means that this fit is just as good as the briefly mentioned triple Gaussian fit. The fit for the Bragg peak in water shows the smallest error and what is curious is that the larger the distance between another Bragg peak to the Bragg peak to water gets, the larger the error gets.

### 3.2 $\Delta R$

The difference that shows up in table 4 for the parameters for lung also shows in the figure 6. The Bragg peak in lung has a lower maximum and is more spread out. The rest of the Bragg peaks seem to have the same shape and this is also what was most likely from the parameters from table 4. The distances between the Bragg peaks are now measured by comparing the  $x$ -values for percentages of the maximum of the function. These results are shown in table 6 and figure 7.

Table 6: Differences (in mm) between the Bragg peak in water and Bragg peak in different materials.

	$\Delta R_{\text{fat}}$	$\Delta R_{\text{bone}}$	$\Delta R_{\text{solidwater}}$	$\Delta R_{\text{aluminium}}$	$\Delta R_{\text{lung}}$
Max data	1.200	-7.800	-0.200	-9.800	26.600
Max fit	1.183	-7.805	-0.233	-9.707	26.692
90% fit	1.199	-7.803	-0.217	-9.700	27.030
80% fit	1.209	-7.802	-0.210	-9.695	27.173
70% fit	1.216	-7.802	-0.206	-9.692	27.289
60% fit	1.225	-7.800	-0.201	-9.687	27.397
50% fit	1.232	-7.800	-0.197	-9.684	27.503
40% fit	1.276	-7.764	-0.157	-9.644	27.648
10% fit	1.279	-7.798	-0.174	-9.662	28.085
1% fit	1.322	-7.804	-0.154	-9.641	28.594

The change in  $\Delta R$  is shown best by taking one of the  $\Delta R$  values as a reference. In table 7 and figure 8 the value of  $\Delta R - \Delta R_{80\%}$  is shown.

Table 7:  $\Delta R - \Delta R_{80\%}$  for all materials compared to water.

Relative height	Fat	Bone	Solid water	Aluminium	Lung
100%	-0.026	-0.003	-0.023	-0.012	-0.481
90%	-0.010	-0.001	-0.007	-0.005	-0.143
70%	0.007	0.000	0.004	0.003	0.116
60%	0.016	0.002	0.009	0.008	0.224
50%	0.023	0.002	0.013	0.011	0.330
40%	0.067	0.038	0.053	0.051	0.475
10%	0.070	0.004	0.036	0.033	0.912
1%	0.113	-0.002	0.056	0.054	1.421

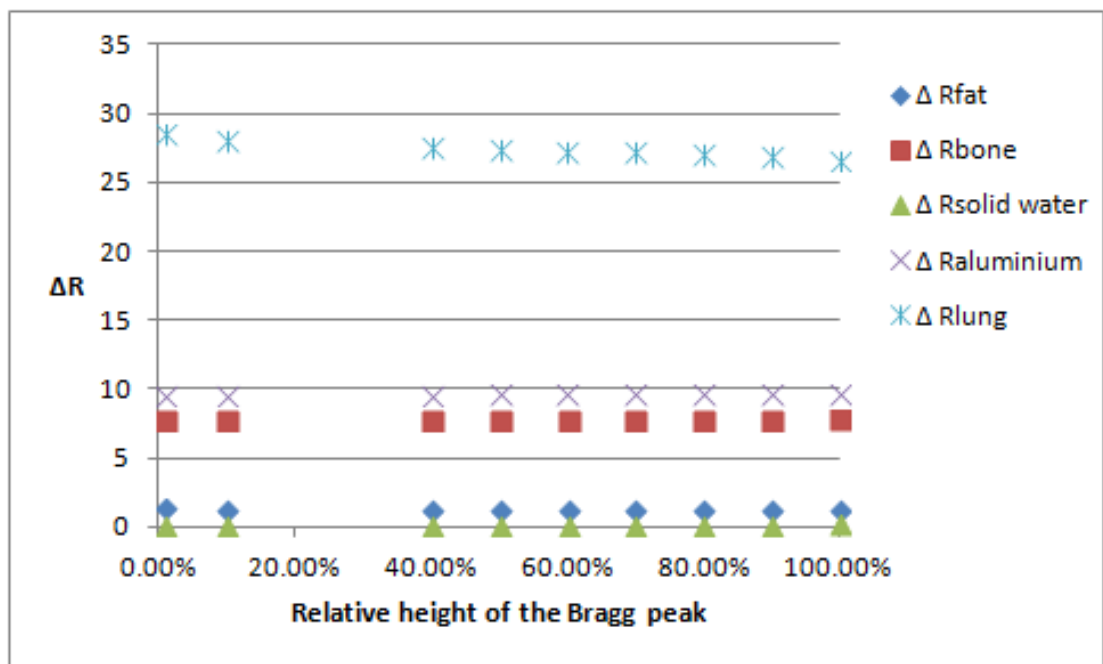


Figure 7: Absolute values of  $\Delta R$  (mm) for all 5 materials from table 6 plotted against the relative height of the Bragg peak.

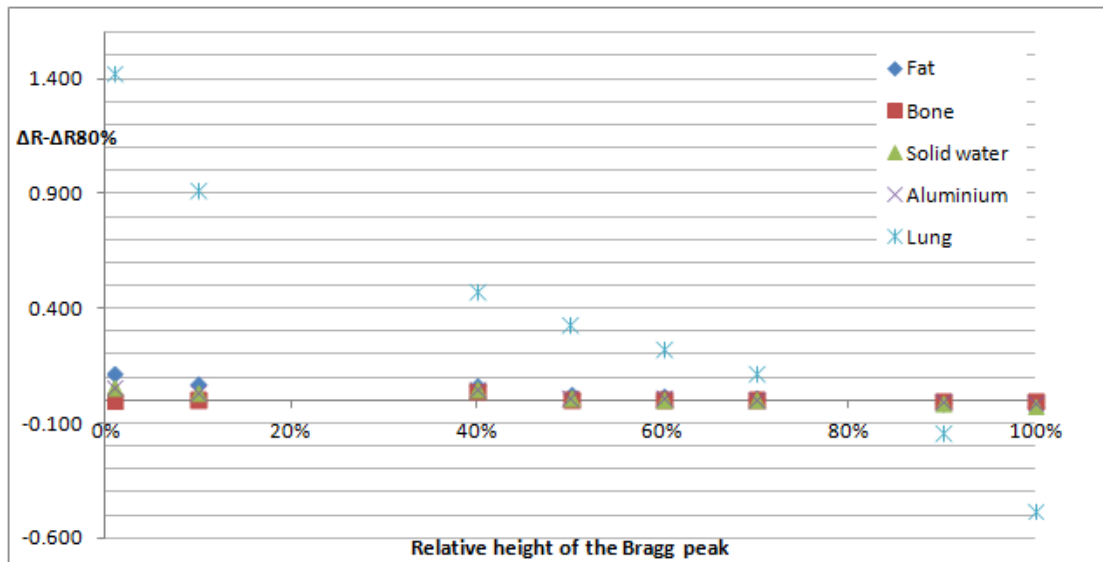


Figure 8:  $\Delta R - \Delta R_{80\%}$  for all materials compared to water plotted against the relative height of the Bragg peak.



## 4 Discussion and conclusions

One important aspect that should be taken into account when analysing the results is the difference in sample thickness used in the measurements. Therefore no strong statements about the effect of the height at which the distance between Bragg peaks is determined can be made based on this comparison alone.

Furthermore it should be clear that the samples used is in fact not real human tissue but only materials that behave the same in a CT scan. A comparison of the composition of these materials shown by Abbema [1] and the actual tissue they are supposed to resemble [3] show that the composition is quite different. This could cause some unexpected results in the Bragg peak profiles and therefore the dependency of  $\Delta R$  on height of the Bragg peak.

Based on the results for  $\Delta R$  the question whether  $\Delta R$  depends on the chosen height of the Bragg peak to measure the distance can be answered. The range difference between Bragg peaks in table 6 shows that there is indeed a difference in  $\Delta R$  when measuring at a different height. This difference is clearly shown in figure 8 and figure 7 and 8 show an opposite trend in height dependency of  $\Delta R$  for materials with a smaller density than water compared to materials with a larger density than water. For lower density materials  $\Delta R$  decreases with height, while for higher density materials  $\Delta R$  increases with height of of the Bragg peak. The height dependency of  $\Delta R$  can most clearly be seen for lung in figure 8. Here it can be seen that the height of the Bragg peak at which  $\Delta R$  is determined can result in a difference of almost 2mm. This dependency is less clear for other materials, but even here the previously mentioned tendency is visible. The greater the difference in density of the material with water is, the greater the height dependency of  $\Delta R$  is. The height dependency actually takes on a very systematic form, since Bragg peaks in materials less dense than water (and thus on the right side of water in figure 6) show a larger distance at lower height of the Bragg peak, while this is exactly the other way around for materials that are more dense than water.

What is of course most clear is that the Bragg peak in lung shows the largest height dependency of the distance, amounting to about 1 mm difference at 40% and even 2mm at 1% compared to the maximum height. Lung has, as is also clear, by far the most distant Bragg peak and even with the naked eye a difference in shape is apparent. This difference, a lower maximum and a broader peak, also showed up in the parameters of the fitted function in table 4.

The Bragg peak for lung fits in very well with the height dependency of  $\Delta R$  that is in turn dependent on the difference in mass density. A density smaller than water, such as lung, would result in a more spread out Bragg peak, which is consistent with the observed development of  $\Delta R$ , where  $\Delta R$  grows as the height is lowered. The height dependency of  $\Delta R$  can thus be understood and explained by the density differences between materials. This however does not

help in determining which height is best to determine  $\Delta R$  and it might even be material dependent.

What is clear however is that, especially for materials that differ greatly in density compared to water, the height dependency should be considered. The difference of 2mm that has been observed in this research could very well lead to an incorrectly modelled Bragg peak which could severely hinder accurate treatment planning.

## 5 References

- [1]Abbema, Joanne K. van et al. Relative electron density determination using a physics based parametrization of photon interactions in medical DECT, *Physics in medicine and biology*, 60, 9 ,2015.
- [2]Hammouda, Boualem. Are Bragg peaks Gaussian?, *Journal of research of the national institute of standards and technology*, 119, 2014.
- [3]Indra, Yohannes. A formulation of tissue- and water-equivalent materials using the stoichiometric analysis method for CT-number calibration in radiotherapy treatment planning, *Physics in medicine and biology*, 57, 2012.
- [4]Newhauser, Wayne D. and Rui Zhang. The physics of proton therapy, *Physics in medicine and biology*, 60, 2015.
- [5]Turner, James E. *Atoms, radiation and radiation protection*, WILEY-VCH Verlag GmbH & Co. KGaA, 2007, 109-138.
- [6][Http://www.cancer.net](http://www.cancer.net)